HHS Public Access

Author manuscript

J Neurochem. Author manuscript; available in PMC 2015 October 15.

Published in final edited form as:

J Neurochem. 2007 May ; 101(4): 889–897. doi:10.1111/j.1471-4159.2007.04541.x.

Minimal role for caspase 12 in the unfolded protein response in oligodendrocytes *in vivo*

Ramaswamy Sharma[*] and **Alexander Gow**[*,†,‡]

[*]Center for Molecular Medicine and Genetics, Wayne State University School of Medicine, Detroit, Michigan, USA

[†]Carman and Ann Adams Department of Pediatrics, Wayne State University School of Medicine, Detroit, Michigan, USA

[‡]Department of Neurology, Wayne State University School of Medicine, Detroit, Michigan, USA

Abstract

The unfolded protein response (UPR) is implicated in many neurodegenerative disorders including Alzheimer, Parkinson and prion diseases, and the leukodystrophy, Pelizaeus–Merzbacher disease (PMD). Critical features of degeneration in several of these diseases involve activation of cell death pathways in various neural cell populations, and the initiator caspase 12 has been proposed to play a central role. Accordingly, pharmacological strategies to inhibit caspase 12 activity have received remarkable attention in anticipation of effecting disease amelioration. Our investigation in animal models of PMD demonstrates that caspase 12 is activated following accumulation of mutant proteins in oligodendrocytes; however, eliminating caspase 12 activity does not alter pathophysiology with respect to levels of apoptosis, oligodendrocyte function, disease severity or life span. We conclude that caspase 12 activation by UPR signaling is an epiphenomenon that plays little discernable role in the loss of oligodendrocytes in vivo and may portend the inconsequence of caspase 12 to the pathophysiology of other protein conformational diseases.

Keywords

C/EBP homologous protein; caspase 9; cell stress; myelin; proteolipid protein

The endoplasmic reticulum (ER) serves as the major quality control compartment of the cell in which individual proteins must adopt stable three-dimensional structures before gaining access to other membrane compartments (Hammond and Helenius 1995). Misfolded proteins are retained in the ER and their accumulation triggers an unfolded protein response (UPR). UPR signaling induces molecular chaperone expression to increase protein-folding capacity in the ER, induces ubiquitin-mediated degradation of ER-localized proteins and attenuates global translation to reduce nascent membrane protein synthesis (Schroder and Kaufman 2005). Normally, this pathway acts to alleviate ER stress and promote cell survival; however, if the ER is overwhelmed by accumulating misfolded proteins, the cell is

Address correspondence and reprint requests to Dr Alexander Gow, Center for Molecular Medicine and Genetics, 3216 Scott Hall, 540 E Canfield Ave, Wayne State University School of Medicine, Detroit, MI 48201, USA. agow@med.wayne.edu.

thought to undergo apoptosis by activating caspase 12, which triggers a caspase cascade (Nakagawa *et al.* 2000; Rao *et al.* 2001).

Murine caspase 12 localizes to the cytoplasmic surface of the ER and is activated by ER stress-inducing agents including brefeldin A, thapsigargin and tunicamycin (Nakagawa *et al.* 2000). Prolonged stress releases caspase 12 to the cytoplasm where it activates caspase 9, which in turn activates caspase 3 (Morishima *et al.* 2002). Data from a number of studies demonstrate activation of caspase 12 in ER stress-induced neurodegenerative disorders and several groups have proposed inhibiting caspase 12 as an attractive therapeutic strategy to ameliorate disease (Nakagawa *et al.* 2000; Beesley *et al.* 2001; Cerghet *et al.* 2001; Siman *et al.* 2001; Kouroku *et al.* 2002; Hetz *et al.* 2003).

The UPR is implicated in conformational diseases in the CNS but, arguably, has been characterized in greatest detail *in vivo* using animal models of Pelizaeus–Merzbacher disease (PMD, reviewed by Gow and Sharma 2003). PMD is a progressive, X-linked leukodystrophy caused by mutations in the *PROTEOLIPID PROTEIN 1* (*PLP1*) gene (Gencic *et al.* 1989) which encodes the major structural protein of CNS myelin (Braun 1984). Coding region mutations cause *PLP1* gene products to accumulate in the ER (Roussel *et al.* 1987), leading to activation of the UPR, a caspase cascade and apoptosis (Gow *et al.* 1998; Southwood *et al.* 2002). Indeed, we have demonstrated UPR signaling in animal models and in PMD by the induction of a number of UPR genes, including molecular chaperones and heat shock proteins Erp-59, -72, -99, HSP47 and BiP as well as transcription factors C/EBP homologous protein (CHOP), activating transcription factor 3 and activating transcription factor 4 (Southwood and Gow 2001; Southwood *et al.* 2002).

Herein, we explore the phenotypic and pathologic consequences of eliminating caspase 12 activity in two naturally occurring mouse models of PMD, *myelin-synthesis-deficient* (*msd)* and *rumpshaker* (*rsh)*. We demonstrate induction and activation of caspase 12 in mild and severe forms of disease in *Plp1* mutant mice and we ablate expression of caspase 12 in these animals by breeding with *Caspase 12*$^{-/-}$ mice to generate double-mutant strains. We find that the impact of PLP1 accumulation in the ER of oligodendrocytes is unchecked in double-mutants in terms of the levels of apoptosis, the expression of myelin genes, the severity of disease and the life span of the animals. Thus, we conclude that caspase 12 plays little or no role in the pathophysiology of PMD and is unlikely to serve as a useful drug target.

Methods

Mouse mutants and background strains

We use two naturally occurring mouse mutants to study the UPR *in vivo*. The *msd* mutation is an alanine-to-valine change at amino acid 243 (A243V) in PLP1 (Gencic and Hudson 1990) and causes severe disease with a life span of 3–4 weeks. The *rsh* mutation is an I187T mutation in PLP1 (Schneider *et al.* 1992) and causes mild disease with a normal life span compared with controls. These animals are excellent models of PMD and the specific mutations have direct correlates in humans (Kobayashi *et al.* 1994; Yamamoto *et al.* 1998). For this study, the *msd* and *rsh* mice have been maintained in a B6C3.F1 (Taconic Farms) background for 10 generations. The *Caspase 12*$^{-/-}$ mice obtained from Dr Yuan (Harvard

Medical School, Boston, MA, USA) were initially on a C57Bl/6 background and were intercrossed with the *msd* and *rsh* mice and maintained in this mixed strain background.

Immunocytochemistry

Anaesthetized mice are perfused intracardially for 15 min with 4% paraformaldehyde in 0.1 mol/L sodium phosphate, pH 7.2. Dissected brains are infiltrated with 25% sucrose in phosphate buffer and embedded in optimal cutting temperature medium. Cryostat sections are permeabilized with methanol for 10 min, blocked in 2% goat serum in Tris–buffered saline (TBS), pH7.5, containing 1% bovine serum albumin and 0.1% gelatin (TBSGBA). Overnight primary antibodies: Rat anti-PLP1/DM-20 (1 : 50, hybridoma AA3 Yamamura *et al.* 1991); Rat anti-caspase 12 (1 : 50; Sigma, St Louis, MO, USA); Rabbit anti-cleaved caspase 12 (1 : 100, D341, Fujita *et al.* 2002), Rabbit anti-cleaved caspase 3 (0.3 μg/mL; Neuromics, Northfield, MN, USA); Mouse anti-myelin basic protein (MBP) (1 : 10 000, Sternberger Monoclonals, Lutherville, MD, USA). Secondary/tertiary reagents: (Rabbit anti-Rat-FITC; Vector Labs, Burlingame, CA, USA); Goat anti-Rabbit-biotin; Jackson Immunoresearch Labs, Westgrove, PA, USA); streptavidin-Texas Red; Vectashield (Vector Labs, Burlingame, CA, USA). Sections are visualized using a Leica DMRA2 microscope (Leica Microsystems, Chatsworth, CA, USA).

Generation of *Caspase 12*$^{-/-}$: *msd/Y* and *Caspase 12*$^{-/-}$: *rsh* mice

Caspase 12$^{-/-}$ mice (Nakagawa *et al.* 2000) were bred with *msd/X* and *rsh/X* carrier females to generate animals for breeding: *Caspase 12*$^{+/-}$ *: msd/X*, *Caspase 12*$^{+/-}$ *: rsh/X* and *Caspase 12*$^{+/-}$ *: X/Y*. Sibling matings of these mice yielded mutant mice expressing *Caspase 12* (*Caspase 12*$^{+/+}$ *: msd/Y* and *Caspase 12*$^{+/+}$ *: rsh/Y*) or lacking a functional *Caspase 12* (*Caspase 12*$^{-/-}$ *: msd/Y* and *Caspase 12*$^{-/-}$ *: rsh/Y*). Carrier females expressing *Caspase 12* were mated with wild-type males to generate the *Caspase 12*$^{+/+}$ colony; carrier females lacking *Caspase 12* were sibling mated with male littermates to generate the *Caspase 12*$^{-/-}$ colony. Matings from *Caspase 12*$^{+/-}$ *: rsh/X* and *Caspase 12*$^{+/-}$ *: X/Y* mice were used to generate a small cohort of wild-type and double-mutant males (i.e. *Caspase 12*$^{+/+}$ *: X/Y*, *Caspase 12*$^{+/+}$ *: rsh/Y* and *Caspase 12*$^{-/-}$ *: rsh/Y*) from the same litter. Mice were genotyped by PCR using phenol : chloroform purified tail DNA (Nakagawa *et al.* 2000; Southwood *et al.* 2002).

Northern blots

Spinal cords were rapidly dissected and stored −80° C. Spinal cord RNA was extracted using the Qiagen RNeasy Lipid Tissue Mini Kit (Qiagen, Valencia, CA, USA). RNA (10 μg) from at least three animals per genotype per age were used per probe per blot. RNA samples were run on 1% formaldehyde-agarose gels as described previously (Southwood *et al.* 2002). Probes used: *Caspase 12*, *Chop*, *Plp1*, *Mbp* and *Gapdh* with washing to 60° C for 15 min with 0.2× SSPE/0.1% sodium dodecyl sulfate. Bands are scanned and quantified as average intensity values measured in Adobe Photoshop 7.0 (Adobe, CA, USA).

Western blots

Frozen spinal cords were homogenized in 200 μL lysis solution (2 mmol/L EDTA, 2% Triton X-100, 0.5 mmol/L phenyl-methylsulfonyl fluoride and protease inhibitors in TBS). Protein concentrations (Biorad, Hercules, CA, USA) were determined and samples stored at −80° C. For immunoblotting, 200 μg of protein was run on 12% polyacrylamide gels (Laemmli 1970), transferred to nitrocellulose (Schleicher and Schuell, Whatman, NJ, USA), blocked with 5% non-fat dry-milk (Carnation, Nestle, Vevey, Switzerland) and probed with primary antibody in 3% non-fat dry-milk at 4° C overnight. Primary antibodies: Rb anti-CHOP (1 : 3000, Rabbit B1259), Mouse anti-MBP (1 : 10 000, Sternberger, Lutherville, MD, USA), Rat anti-PLP1/DM-20 (1 : 50, AA3), Rabbit anti-caspase 12 (1 : 3000, Neuromics, Northfield, MN, USA) and Mouse anti-caspase 9 (1 : 1000, Cell Signaling, Danvers, MA, USA). Biotinylated secondary antibodies and alkaline phosphatase-strept-avidin (1 : 2000, Jackson Immunoresearch Labs, Westgrove, PA, USA) are used. Loading controls: blots are stripped at 55° C for 30 min (62.5 mmol/L Tris–HCl, pH, 2% SDS, 100 mmol/L β-mercaptoethanol) and re-probed for β-actin (1: 5000; Sigma).

TUNEL labeling

Transverse cryostat sections of C1 spinal cord from perfused mice are terminal dUTP nick-end labeling (TUNEL)-labeled using the In situ Cell Death Detection kit, TMR red (Roche, Indianapolis, IN, USA). A minimum of three slides per animal (three sections per slide) from three different animals per genotype are used. Sections are overlaid with 30 μL of reaction mixture and incubated in a humidified chamber for 30 min at 37° C (Gow *et al.* 1998). Sections are incubated in 4′,6-diamidino-2-phenylindole (DAPI), and counted. The data are expressed as numbers of apoptotic cells per 10 μm cryostat section. Spinal cord regions are matched in all animals to ensure the same area of tissue in each animal and we assume that the total number of nuclei per section is similar in all treatment groups. Previous studies indicate that the number of differentiating oligodendrocytes in *Plp1* mutant mice (Ghandour and Skoff 1988) is similar to that in wild-type mice beyond P16.

Assay for DEVDase activity

Mouse optic nerves are rapidly dissected and stored at −80° C. Samples are homogenized (50 μL per nerve; 0.5% NP-40, 0.5 mmol/L EDTA, 150 mmol/L NaCl, 50 mmol/L Tris, pH 7.5, 0.5 mmol/L phenylmethylsulfonyl fluoride and protease-inhibitors), kept on ice for 30 min, sonicated and centrifuged at 15 000 *g* for 10 min at 4° C. In a 96-well plate, 50 μL of supernatant (approximately 80 μg of protein) is mixed with 100 μL of 2× Reaction Buffer (20 mmol/L HEPES, pH 7.5, 0.05 mol/L NaCl, 2.5 mmol/L dithiothreitol), 50 μmol/L (200×) Ac-DEVD-AMC substrate (Bio-source International, Camarillo, CA, USA) and water to 200 μL. Caspase 3 inhibitor III (Calbiochem, San Diego, CA, USA) is added to 1 μmol/L final. Pure AMC (1 μmol/L) is the positive control. Rate reactions are performed at 37° C and fluorescence measured using a SPECTRA®max GEMINI plate reader (Molecular Devices Corporation, Sunnyvale, CA, USA) with excitation/emission wavelengths of 355/460 nm and a cut-off at 435 nm. Averaged fluorescence from triplicate assays are normalized against wild-type littermates. Experiments are repeated three times.

Rotarod tests

At least 10 animals from four genotypes (*Caspase 12*$^{+/+}$: *X/Y*, *Caspase 12*$^{+/+}$: *rsh/Y*, *Caspase 12*$^{-/-}$: *X/Y* and *Caspase 12*$^{-/-}$: *rsh/ Y*) were tested for changes in motor capacity using an ENV-577 mol/L rotarod (Med Associates, Georgia, VT, USA). Mice were examined at P50, P100, P180 and P300 as described (Gow *et al.* 1999).

Longevity

Cohorts of at least twenty mice per genotype (*Caspase 12*$^{+/+}$: *X/Y*, *Caspase 12*$^{+/+}$: *msd/Y*, *Caspase 12*$^{-/-}$: *X/Y* and *Caspase 12*$^{-/-}$: *msd/Y*, *Caspase 12*$^{+/+}$: *X/Y*, *Caspase 12*$^{+/+}$: *rsh/Y*, *Caspase 12*$^{-/-}$: *X/Y* and *Caspase 12*$^{-/-}$: *rsh/Y*) were analyzed using a Kaplan–Meier survival analysis up to 12 months to compare the life spans of mutants and littermate controls.

Statistical analyses

A non-parametric two-tailed Mann–Whitney test (GraphPad Software, San Diego, CA, USA) was used to evaluate the longevity studies. For all other analyses, the Kruskal–Wallis test (non-parametric ANOVA) with a Tukey post-test was used. In TUNEL analyses using three mice per genotype, we have at least 80% power to detect a 33% change in the number of apoptotic nuclei between *Chop*$^{+/+}$: *rsh/Y* versus *Chop*$^{-/-}$: *rsh/Y* and between *Chop*$^{+/+}$: *msd/*Y versus *Chop*$^{-/-}$: *msd/*Y at a significance level of 0.05 (two-tailed *t*-tests).

Results

Caspase 12 is activated in *Plp1* mutant mice

Caspases exist in the cell as inactive zymogens and require cleavage to form active heterotetramers. Cleavage sites in pro caspase 12 include an autoprocessing site at D^{318} (Fujita *et al.* 2002) and the p20/p10 cleavage site at D^{341} (Rao *et al.* 2001). Using an antibody that detects the D^{341} cleavage, immunolabeling brainstems from post-natal day 16 (P16) wild-type and *msd* mice reveals activated caspase 12 in the cytoplasm of a sub-population of PLP1^{+} oligodendrocytes in mutant (Figs 1d–f) but not wild-type mice (Figs 1a–c). Labeling of *rsh/Y* sections shows similar caspase 12 activation (data not shown). The nuclei of these double-positive cells are condensed, as indicated by DAPI staining, which is confirmed apoptosis by TUNEL labeling in conjunction with activated caspase 12 labeling (Figs 1g–i). Indeed, 100% of D^{341}-positive oligodendrocytes are TU-NEL-positive. Together, these data show that caspase 12 is activated in apoptotic mature oligodendrocytes from *Plp1* mutant mice but not from wild-type mice.

Characterization of *Caspase 12* $^{-/-}$ double mutants

Caspase 12$^{-/-}$ mice were generated previously by replacing portions of intron 4 and exon 5 of the *Caspase 12* gene with a *PGK-neo* cassette on the non-coding strand (Nakagawa *et al.* 2000). These mice were intercrossed with *msd/X* and *rsh/X* carrier females for two generations to yield separate Caspase 12$^{+/+}$ and Caspase 12$^{-/-}$ double-mutant colonies for experimentation. In addition, a small cohort of mutant mice were generated by breeding *Caspase 12*$^{+/-}$: *X/Y* with *Caspase 12*$^{+/-}$: *msd/X* or *Caspase 12*$^{+/-}$: *rsh/X* mice. Mutant

genotypes are identified by PCR (Fig. 2a). Characterization of these animals at P16 by northern (Fig. 2b) and western blotting (Fig. 2c) shows that caspase 12 expression is induced in *msd/Y* and *rsh/Y* mutants compared with controls and that caspase 12 is absent in all *Caspase 12*$^{-/-}$ mice. Finally, labeling with antibodies against caspase 12 shows the presence of this protein in the cytoplasm of many *Caspase 12*$^{+/+}$: *msd/Y* cells but not in cells from *Caspase 12*$^{-/-}$: *msd/Y* mice.

No change in apoptosis in the *Caspase 12* $^{-/-}$ double mutants

To examine the effect of ablating *Caspase 12* on cell death in *Plp1* mutant mice, we performed TUNEL labeling on cervical spinal cords from P16 *Caspase 12*$^{-/-}$: *msd/Y* and *Caspase 12*$^{-/-}$: *rsh/Y* mice and littermate controls. Predictions in the literature that blocking caspase 12 activity is neuroprotective (Nakagawa *et al.* 2000; Hetz *et al.* 2003) suggest that double-mutant mice should exhibit lower levels of apoptosis than *Plp1* single mutant animals.

In *Caspase 12*$^{+/+}$: *msd/Y* mice, (Fig. 3c) we observe increased numbers of apoptotic cells compared with controls (Fig. 3a). A similar increase is observed in *Caspase 12*$^{-/-}$: *msd/Y* mice and is approximately six-fold (Table 1). In addition, we observe increased apoptosis in *rsh/Y* mice with and without caspase 12 approximating three-fold above controls. An ANOVA of the data in Table 1 indicates that the number of apoptotic cells in *Caspase 12*$^{+/+}$: *msd/Y* versus *Caspase 12*$^{-/-}$: *msd/Y* mice is not statistically significant ($p > 0.05$) and a similar result is found for *Caspase 12*$^{+/+}$: *rsh/Y* versus *Caspase 12*$^{-/-}$ *: rsh/Y* mice ($p > 0.05$). In contrast, levels of apoptosis are significantly increased in all double mutants compared with control mice ($p < 0.05$). Thus, levels of apoptosis associated with the pathophysiology of *Plp1* mutations are independent of caspase 12 activity.

In select cases, genetic background has been suggested to influence disease severity in animal models of PMD (Al-Saktawi *et al.* 2003) which, technically, could bias our analysis of *Caspase 12*$^{+/+}$ and *Caspase 12*$^{-/-}$ colonies. Accordingly, we generated littermate *rsh/Y* mice (two animals per genotype) with or without a functional *Caspase 12* gene from *Caspase 12*$^{+/-}$: *rsh/X* and *Caspase 12*$^{+/-}$: *X/Y* breeding pairs for analysis using TUNEL labeling. Levels of apoptosis in the spinal cords of these animals are similar to the data in Table 1 and we conclude there is no evidence to suggest that genetic background is a confounding factor in our analysis.

Effector caspases are activated in *Caspase 12*$^{-/-}$ *: msd/Y* mice

Caspase 12 is regarded as a UPR-specific initiator caspase that triggers a canonical caspase cascade by activating caspase 9, which in turn activates the executioner caspase 3 (Morishima *et al.* 2002). However, the similarity in apoptosis levels of *Plp1* mutant mice in the presence and absence of caspase 12 suggests a canonical caspase cascade is occurring in the double mutants. To explore this possibility, we examined the activities of caspase 9 and -3 in the *Plp1* mutants.

Western blots of spinal cord from P16 *Plp1* mutant mice are shown in Fig. 4a. In control mice, caspase 9 is detected at low levels independent of caspase 12 activity. However,

caspase 9 is strongly increased in *msd/Y* mice, which is indicative of higher activity (Stennicke *et al.* 1999), and this increase is independent of caspase 12 activity.

To determine if caspase 3 is activated in *msd/Y* mice in the absence of caspase 12, we labeled brain sections with antibodies against activated caspase 3. Arrowheads show apoptotic oligodendrocytes with condensed nuclei strongly labeled with caspase 3 antibodies, which demonstrates that a caspase cascade is in progress in the presence (Fig. 4b) and absence (Fig. 4c) of caspase 12. We also examined caspase 3 activity directly in optic nerves from *Plp1* mutant mice using a DEVDase-activity assay. DEVD-AMC (Asp-Glu-Val-Asp-AMC) is preferentially cleaved by caspase 3 with the release of an AMC moiety that is detected fluorometrically. In Table 2, DEVDase activity is summarized as fold-change above control (*Caspase 12*$^{+/+}$: *X/Y*) levels for *msd/Y* and *rsh/Y* mice in the presence and absence of caspase 12. All *Plp1* mutant samples exhibit approximately five-fold greater DEVDase activity than control mice and addition of a competitive inhibitor abolishes caspase activity. Thus, again, our data are indicative of a UPR-induced caspase cascade that is independent of caspase 12.

No changes in expression of myelin genes

Northern blots from P16 spinal cord show induced expression of the *Chop* gene compared with controls, which demonstrates a UPR in *msd/Y* and *rsh/Y* mice that is similar in the presence or absence of caspase 12 activity (Fig. 5a). To determine if the absence of caspase 12 has consequences on oligodendrocyte function, we examined expression of the two most abundant myelin gene products, PLP1 and MBP. Expression of *Plp1* and *Mbp* mRNAs is reduced in the mutants compared with controls, which is an expected consequence of hypomyelination (Gardinier and Macklin 1988; Mitchell *et al.* 1992). However, there are no major differences in steady-state mRNA levels for these genes in the presence or absence of caspase 12. Figure 5b shows steady state levels of UPR and myelin proteins in spinal cord samples. Consistent with the northern blots, CHOP levels are significantly elevated in the *Plp1* mutants but the induction is independent of caspase 12. Thus, *Chop* expression levels are not influenced by caspase 12 activity. The same is true in *rsh*/ Y mice for levels of the two *Plp1* gene products, PLP1 and DM-20, and the four MBP isoforms. In *msd/Y* mice, levels of PLP1 and DM-20 are too low to detect by western blotting and MBP is unaffected by the absence of caspase 12. Together, these data show that a lack of caspase 12 activity does not confer significant neuroprotection on *Plp1* mutant mice, at least in terms of oligodendrocyte survival that would lead to increased CNS myelination, increased steady state levels of myelin proteins and, presumably, amelioration of disease severity.

Loss of caspase 12 has no effect on rotarod performance

As a further test of any potential neuroprotective effects associated with deletion of the *Caspase 12* gene, we subjected *rsh/Y* mice and controls to rotarod analysis at four different ages between 2 and 12 months of age. Rotarod tests are commonly used as sensitive but indirect measures of motor coordination in the CNS. As shown in Fig. 6, the *Caspase 12*$^{+/+}$: *rsh/Y* and *Caspase 12*$^{-/-}$: *rsh/Y* mutant cohorts perform poorly in this analysis at early ages compared with controls but eventually are indistinguishable from controls (at P300). More importantly, these mutant cohorts are indistinguishable at all timepoints (open vs. closed

triangles). Thus, the lack of caspase 12 activity is of little consequence to pathophysiology and does not appear to be neuroprotective. Curiously, we find that wild-type mice (*Caspase* $12^{+/+}$: *X/Y*) perform poorly at P180 compared with their *Caspase* $12^{-/-}$: *X/Y* counterparts. This striking difference is transient, because the two genotypes perform similarly at other timepoints ($p > 0.05$), and we suspect may reflect a spurious result. We did not find any differences in animal weights between the two groups and we could not identify any other obvious physiological causes.

No change in life span of *Caspase* $12^{-/-}$: *msd/Y* and *Caspase* $12^{-/-}$: rsh/Y mice

A final test of the role of caspase 12 in the pathophysiology of *Plp1* mutations is the resulting life span of double-mutant mice compared with controls. Kaplan–Meier analyses of more than 20 mice per genotype are shown in Fig. 7 for *msd/ Y* and *rsh/Y* mice in the presence and absence of *Caspase 12*. In Fig. 7a, all control mice with or without *Caspase 12* survive the 60 day analysis. In contrast, *Caspase12*$^{+/+}$: *msd/Y* mice begin to die around P24 and all mice in this cohort are dead by P30. These data are consistent with previous studies (Billings-Gagliardi *et al.* 1980). Survival of the *Caspase* $12^{-/-}$: *msd/Y* cohort is indistinguishable from *msd/Y*, indicating that the absence of caspase 12 does not change the phenotype. In Fig. 7b, essentially all mice survive the 300-day analysis, which demonstrates that the absence of caspase 12 does not have a detrimental effect on the survival of *rsh/Y* mice. Thus, these data demonstrate that ablating *Caspase 12* does not confer neuroprotection in *Plp1* mutant mice.

Discussion

Caspases have emerged as promising therapeutic targets for the amelioration of a number of neurodegenerative disorders. For example, animal models of Huntington disease which express dominant negative caspase 1 exhibit delayed onset of disease, and intracerebroventricular administration of the zVAD-fmk pancaspase inhibitor also delays mortality (Ona *et al.* 1999). Similarly, inhibiting caspase 1 provides neuro-protection in animal models of Parkinson disease (Klevenyi *et al.* 1999). Caspase 12 mediates ER stress-specific apoptosis (Nakagawa *et al.* 2000), and inhibiting caspase 12 may be an important neuroprotective strategy. Thus, over-expressing dominant-negative caspase 12 in prion-infected N2A cells diminishes apoptosis (Hetz *et al.* 2003). Primary cortical neurons treated with antisense *Caspase 12* prior to β-amyloid exposure are resistant to apoptosis (Nakagawa *et al.* 2000). However, most caspase 12 inhibition studies have been performed *in vitro* and consequences on the pathophysiology of UPR-induced diseases *in vivo* are unknown.

Herein, we evaluate neuroprotection *in vivo* by inhibiting caspase 12 in two naturally occurring mouse models of PMD for which ER stress-induced apoptosis is a primary feature of the phenotype. Contrary to the results of *in vitro* studies, we find that the absence of caspase 12 activity does not protect oligodendrocytes undergoing UPR-induced apoptosis and does not positively (or negatively) impact prognosis, oligodendrocyte function or life span of *Plp1* mutant mice. Thus, induction and activation of caspase 12 in *msd/Y* and *rsh/Y* mice is likely an epiphenomenon associated with the pathophysiology rather than a root cause of neurodegeneration.

The absence of a demonstrable effect from gene ablation studies implies the existence of a compensatory mechanism. The fact that the caspase family encompasses more than 10 family members with significant levels of overlap in substrate binding suggests that another caspase in oligodendrocytes performs the function of caspase 12 in our double-mutant mice. Which caspase might this be?

The *CASPASE 12* gene does not yield a functional protein in most human populations, indicating that evolution over the last 100–500 thousand years has selected against this gene (Fischer *et al.* 2002; Xue *et al.* 2006). Accordingly, we might anticipate the ascension of another caspase to usurp caspase 12 function, or the expanded function of an existing caspase. Several lines of evidence suggest that caspase 4 replaces caspase 12 function in humans (Hitomi *et al.* 2004). For example, human caspase 4 shares 48% identity with murine caspase 12. The genes encoding these proteins form a cluster comprising *CASPASE 1, -5, -4 and -12* on chromosome 11q22.3 in a region syntenic to mouse chromosome 9 containing the *Caspase 1, -11 and -12* gene cluster. Thus, caspase 4 may have arisen from a duplication of caspase 12 within the last 75 million years. However, caspase 4 has been shown *in vitro* not to play a significant role in UPR-induced apoptosis (Obeng and Boise 2005; Di Sano *et al.* 2006).

The *Caspase 11* gene, which is physically located within a few kilobases of *Caspase 12* in mice, also has been linked to UPR-induced apoptosis (Endo *et al.* 2006). However, Nicholson and colleagues (Saleh *et al.* 2006) have recently suggested that the *Caspase 11* gene is not expressed in the *Caspase 12* knockout mice (Nakagawa *et al.* 2000) used in the current study, and that this mutant strain is functionally a *Caspase 12 : Caspase 11* double knockout. If so, our data indicate that the absence of both of these caspases in the *msd/ Y* and *rsh/Y* backgrounds fails to confer protection from apoptosis. Thus, neither caspase 12 nor caspase 11 play significant roles in UPR-induced cell death. In this light, our data cast some doubt on the existence of a UPR-specific enzyme that serves as a restriction point for ER-associated apoptotic death signals. Rather, other caspases that respond to a broader range of signals may be involved.

In the absence of caspase 12, how are caspases 9 and 3 activated in *msd/Y* and *rsh/Y* mice? Currently, we cannot rule out the possibility that caspase 8 is activated during ER stress as has been suggested from *in vitro* studies (Jimbo *et al.*, 2003). Caspase 8 could then activate caspase 3 directly and induce the cleavage of Bid-to-tBid, which would effect mitochondrial permeabilization, release of cytochrome *c* and activation of caspase 9. Currently, this hypothesis cannot be tested because of the lack of commercial reagents with sufficient sensitivity *in vivo.*

A surprising outcome in the current study is our finding of increased levels of apoptosis in *rsh/Y* (*Caspase* $12^{+/+}$) mice compared with controls (Table 1). Previous studies (Fanarraga *et al.* 1992; Mitchell *et al.* 1992; Schneider *et al.* 1992) have claimed that apoptosis is not a feature of the pathophysiology in *rsh/Y* mice. To the contrary, we have confirmed our morphometric findings in several sub-colonies of *rsh/Y* mice maintained over 4 years (data not shown) and these data are consistent with our DEVDase assays (Table 2), which reveal higher levels of caspase activity in *rsh/Y* mice. Furthermore, we note corroborating data

from Billings-Gagliardi *et al.* 2001. Importantly, the three-fold higher-than-normal levels of apoptosis measured for *rsh/Y* in the current study is significantly less than the five-fold higher levels we observe in *Chop*$^{-/-}$: *rsh/Y* mice which is consistent with exacerbation of the behavioral phenotype in the double mutants (Southwood *et al.* 2002).

Irrespective of the increase in apoptosis observed in *rsh/Y* mice during development, cell death in these animals is insufficient to deplete oligodendrocyte progenitor pools and *rsh/Y* mice eventually myelinate the CNS to a large extent, which ameliorates their phenotype (Fig. 6). Importantly, these data suggest that curbing apoptosis will positively impact PMD.

Acknowledgments

We thank Dr J. Yuan, Department of Cell Biology, Harvard Medical School, Boston, MA, USA for the *Caspase 12*$^{-/-}$ mice and Dr T. Momoi, National Institute of Neuroscience, Tokyo, Japan, for antibodies against activated caspase 12 (D^{341}). This work has been supported by grants to A.G. from NINDS, NIH (NS43837) and the National Multiple Sclerosis Society (RG2891).

Abbreviations used

CHOP	C/EBP homologous protein
DAPI	4′,6-diamidino-2-phenylindole
ER	endoplasmic reticulum
PMD	Pelizaeus–Merzbacher disease
PLP1	proteolipid protein 1
TUNEL	terminal dUTP nick-end labeling
UPR	unfolded protein response

References

Al-Saktawi K, McLaughlin M, Klugmann M, Schneider A, Barrie JA, McCulloch MC, Montague P, Kirkham D, Nave KA, Griffiths IR. Genetic background determines phenotypic severity of the Plp rumpshaker mutation. J Neurosci Res. 2003; 72:12–24. [PubMed: 12645075]

Beesley JS, Lavy L, Eraydin NB, Siman R, Grinspan JB. Caspase-3 activation in oligodendrocytes from the myelin-deficient rat. J Neurosci Res. 2001; 64:371–379. [PubMed: 11340644]

Billings-Gagliardi S, Adcock LH, Wolf MK. Hypomye-linated mutant mice: description of jp^{msd} and comparison with jp and qk on their present genetic backgrounds. Brain Res. 1980; 194:325–338. [PubMed: 7388618]

Billings-Gagliardi S, Nunnari JJ, Wolf MK. Rumpshaker behaves like juvenile-lethal Plp mutations when combined with shiverer in double mutant mice. Dev Neurosci. 2001; 23:7–16. [PubMed: 11173922]

Braun, PE. Molecular organization of myelin. In: Morell, P., editor. Myelin. Plenum Press; New York: 1984. p. 97-116.

Cerghet M, Bessert DA, Nave KA, Skoff RP. Differential expression of apoptotic markers in jimpy and in Plp overexpressors: evidence for different apoptotic pathways. J Neurocytol. 2001; 30:841–855. [PubMed: 12165674]

Di Sano F, Ferraro E, Tufi R, Achsel T, Piacentini M, Cecconi F. Endoplasmic reticulum stress induces apoptosis by an apoptosome-dependent but caspase 12-independent mechanism. J Biol Chem. 2006; 281:2693–2700. [PubMed: 16317003]

Endo M, Mori M, Akira S, Gotoh T. C/EBP homologous protein (CHOP) is crucial for the induction of caspase-11 and the pathogenesis of lipopolysaccharide-induced inflammation. J Immunol. 2006; 176:6245–6253. [PubMed: 16670335]

Fanarraga ML, Griffiths IR, McCulloch MC, Barrie JA, Kennedy PG, Brophy PJ. Rumpshaker: an X-linked mutation causing hypomyelination: developmental differences in myelination and glial cells between the optic nerve and spinal cord. Glia. 1992; 5:161–170. [PubMed: 1375190]

Fischer H, Koenig U, Eckhart L, Tschachler E. Human caspase 12 has acquired deleterious mutations. Biochem Biophys Res Commun. 2002; 293:722–726. [PubMed: 12054529]

Fujita E, Kouroku Y, Jimbo A, Isoai A, Maruyama K, Momoi T. Caspase-12 processing and fragment translocation into nuclei of tunicamycin-treated cells. Cell Death Differ. 2002; 9:1108–1114. [PubMed: 12232799]

Gardinier MV, Macklin WB. Myelin proteolipid protein gene expression in jimpy and jimpy(msd) mice. J Neurochem. 1988; 51:360–369. [PubMed: 2455772]

Gencic S, Hudson LD. Conservative amino acid substitution in the myelin proteolipid protein of jimpy^{msd} mice. J Neurosci. 1990; 10:117–124. [PubMed: 1688931]

Gencic S, Abuelo D, Ambler M, Hudson LD. Pelizaeus–Merzbacher disease: an X-linked neurologic disorder of myelin metabolism with a novel mutation in the gene encoding proteolipid protein. Am J Hum Genet. 1989; 45:435–442. [PubMed: 2773936]

Ghandour M, Skoff R. Expression of galactocerebroside in developing normal and jimpy oligodendrocytes *in situ*. J Neurocytol. 1988; 17:485–498. [PubMed: 3193128]

Gow A, Sharma R. The unfolded protein response in protein aggregating diseases. Neuromolecular Med. 2003; 4:73–94. [PubMed: 14528054]

Gow A, Southwood CM, Lazzarini RA. Disrupted proteolipid protein trafficking results in oligodendrocyte apoptosis in an animal model of Pelizaeus–Merzbacher disease. J Cell Biol. 1998; 140:925–934. [PubMed: 9472043]

Gow A, Southwood CM, Li JS, Pariali M, Riordan GP, Brodie SE, Danias J, Bronstein JM, Kachar B, Lazzarini RA. CNs myelin and sertoli cell tight junction strands are absent in *Osp/Claudin 11*-Null mice. Cell. 1999; 99:649–659. [PubMed: 10612400]

Hammond C, Helenius A. Quality control in the secretory pathway. Curr Op Cell Biol. 1995; 7:523–529. [PubMed: 7495572]

Hetz C, Russelakis-Carneiro M, Maundrell K, Castilla J, Soto C. Caspase-12 and endoplasmic reticulum stress mediate neurotoxicity of pathological prion protein. Embo J. 2003; 22:5435–5445. [PubMed: 14532116]

Hitomi J, Katayama T, Eguchi Y, et al. Involvement of caspase-4 in endoplasmic reticulum stress-induced apoptosis and Abeta-induced cell death. J Cell Biol. 2004; 165:347–356. [PubMed: 15123740]

Jimbo A, Fujita E, Kouroku Y, Ohnishi J, Inohara N, Kuida K, Sakamaki K, Yonehara S, Momoi T. ER stress induces caspase-8 activation, stimulating cytochrome c release and caspase-9 activation. Exp Cell Res. 2003; 283:156–166. [PubMed: 12581736]

Klevenyi P, Andreassen O, Ferrante RJ, Schleicher JR Jr, Fried-lander RM, Beal MF. Transgenic mice expressing a dominant negative mutant interleukin-1beta converting enzyme show resistance to MPTP neurotoxicity. Neuroreport. 1999; 10:635–638. [PubMed: 10208603]

Kobayashi H, Hoffman EP, Marks HG. The *rumpshaker* mutation in spastic paraplegia. Nat Genet. 1994; 7:351–352. [PubMed: 7522741]

Kouroku Y, Fujita E, Jimbo A, et al. Polyglutamine aggregates stimulate ER stress signals and caspase-12 activation. Hum Mol Genet. 2002; 11:1505–1515. [PubMed: 12045204]

Laemmli UK. Cleavage of structural proteins during the assembly of the head of bacteriophage T4. Nature. 1970; 227:680–685. [PubMed: 5432063]

Mitchell LS, Gillespie SC, McAllister F, Fanarraga ML, Kirkham D, Kelly B, Brophy PJ, Griffiths IR, Montague P, Kennedy PG. Developmental expression of major myelin protein genes in the CNS of X-linked hypomyelinating mutant rumpshaker. J Neurosci Res. 1992; 33:205–217. [PubMed: 1280692]

Morishima N, Nakanishi K, Takenouchi H, Shibata T, Yasuhiko Y. An endoplasmic reticulum stress-specific caspase cascade in apoptosis. Cytochrome c-independent activation of caspase-9 by caspase-12. J Biol Chem. 2002; 277:34 287–34 294.

Nakagawa T, Zhu H, Morishima N, Li E, Xu J, Yankner BA, Yuan J. Caspase-12 mediates endoplasmic-reticulum-specific apoptosis and cytotoxicity by amyloid-beta. Nature. 2000; 403:98–103. [PubMed: 10638761]

Obeng EA, Boise LH. Caspase-12 and caspase-4 are not required for caspase-dependent endoplasmic reticulum stress-induced apoptosis. J Biol Chem. 2005; 280:29 578–29 587.

Ona VO, Li M, Vonsattel JP, et al. Inhibition of caspase-1 slows disease progression in a mouse model of Huntington's disease. Nature. 1999; 399:263–267. [PubMed: 10353249]

Rao RV, Hermel E, Castro-Obregon S, del Rio G, Ellerby LM, Ellerby HM, Bredesen DE. Coupling endoplasmic reticulum stress to the cell death program. Mechanism of caspase activation. J Biol Chem. 2001; 276:33 869–33 874.

Roussel G, Meskovic NM, Trifilieff E, Artault JC, Nussbaum JL. Arrest of proteolipid transport through the Golgi apparatus in Jimpy brain. J Neurocytol. 1987; 16:195–204. [PubMed: 3305791]

Saleh M, Mathison JC, Wolinski MK, Bensinger SJ, Fitzgerald P, Droin N, Ulevitch RJ, Green DR, Nicholson DW. Enhanced bacterial clearance and sepsis resistance in caspase-12-deficient mice. Nature. 2006; 440:1064–1068. [PubMed: 16625199]

Schneider A, Montague P, Griffiths I, Fanarraga M, Kennedy P, Brophy P, Nave KA. Uncoupling of hypomyelination and glial cell death by a mutation in the proteolipid protein gene. Nature. 1992; 358:758–761. [PubMed: 1380672]

Schroder M, Kaufman RJ. ER stress and the unfolded protein response. Mutat Res. 2005; 569:29–63. [PubMed: 15603751]

Siman R, Flood DG, Thinakaran G, Neumar RW. Endoplasmic reticulum stress-induced cysteine protease activation in cortical neurons: effect of an Alzheimer's disease-linked pres-enilin-1 knock-in mutation. J Biol Chem. 2001; 276:44 736–44 743.

Southwood CM, Gow A. Molecular mechanisms of disease stemming from mutations in the proteolipid protein gene. Micros Res Tech. 2001; 52:700–708.

Southwood CM, Garbern J, Jiang W, Gow A. The unfolded protein response modulates disease severity in Pelizaeus–Merzbacher disease. Neuron. 2002; 36:585–596. [PubMed: 12441049]

Stennicke HR, Deveraux QL, Humke EW, Reed JC, Dixit VM, Salvesen GS. Caspase-9 can be activated without proteolytic processing. J Biol Chem. 1999; 274:8359–8362. [PubMed: 10085063]

Xue Y, Daly A, Yngvadottir B, et al. Spread of an inactive form of caspase-12 in humans is due to recent positive selection. Am J Hum Genet. 2006; 78:659–670. [PubMed: 16532395]

Yamamoto T, Nanba E, Zhang H, Sasaki M, Komaki H, Takeshita K. Jimpy(msd) mouse mutation and connatal Pelizaeus–Merzbacher disease. Am J Med Genet. 1998; 75:439–440. [PubMed: 9482656]

Yamamura T, Konola JT, Wekerle H, Lees MB. Mono-clonal antibodies against myelin proteolipid protein: identification and characterization of two major determinants. J Neurochem. 1991; 57:1671–1680. [PubMed: 1717653]

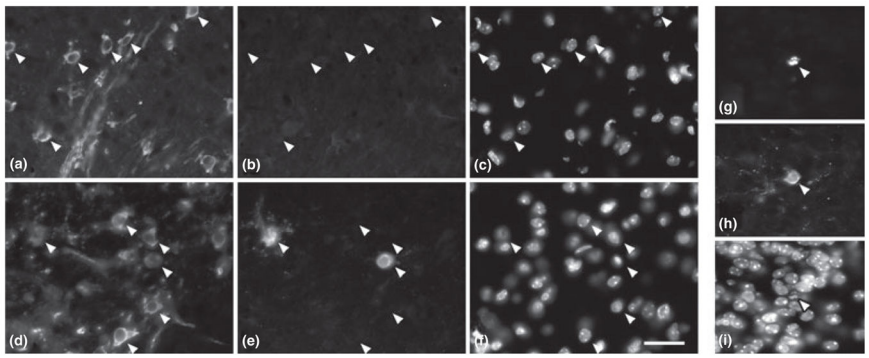

Fig. 1.

Caspase 12 is activated in *msd/Y* mice. Immunolabeling of brainstem from P16 *X/Y* (a, b and c) and *msd/Y* (d, e and f) for PLP1 (a and d) and activated caspase 12 (b and e) shows that activated caspase 12 is present only in oligodendrocytes of *msd/Y* mice. TUNEL staining (g) reveals that apoptotic cells in *msd/Y* mice are positive for activated caspase 12 (h). Nuclei are labeled with DAPI (c, f and i). Scalebar: 30 μm.

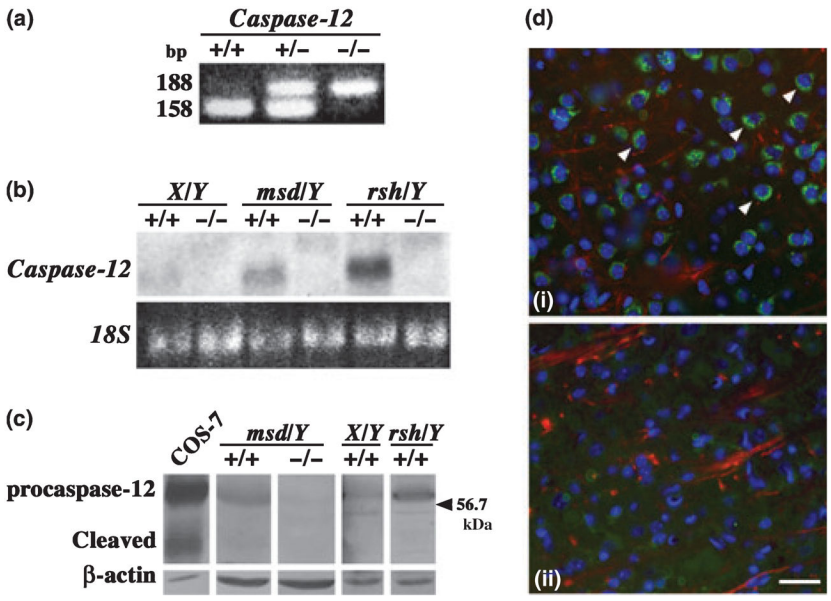

Fig. 2.

Characterization of *Caspase 12* $^{-/-}$ double-mutant mice. (a) PCR identifies wild-type (158 bp) and mutant (188 bp) genotypes (b) northern blots show *Caspase 12* is strongly induced in *msd/Y* and *rsh/Y* mutants compared with *X/Y* and also the absence of *Caspase 12* in the *Caspase 12*$^{-}$/$^{-}$ double mutants. (c) Immunoblots show induction of caspase 12 in Plp1 mutant mice compared *with X/Y* and its absence in *Caspase 12* $^{-}$/$^{-}$ double mutants. Positive control: COS-7 cells transfected with murine *Caspase 12*. Auto-cleavage of caspase 12 upon over-expression has previously been observed (Fujita *et al.* 2002). (d) Immunolabeling of brainstem for MBP (red) and caspase 12 (green) confirms (a) the presence of caspase 12 in *msd/Y* and (b) its absence in the *Caspase 12* $^{-}$/$^{-}$: *msd/Y* mice. Nuclei are stained with DAPI (blue). Scalebar: 25 μm.

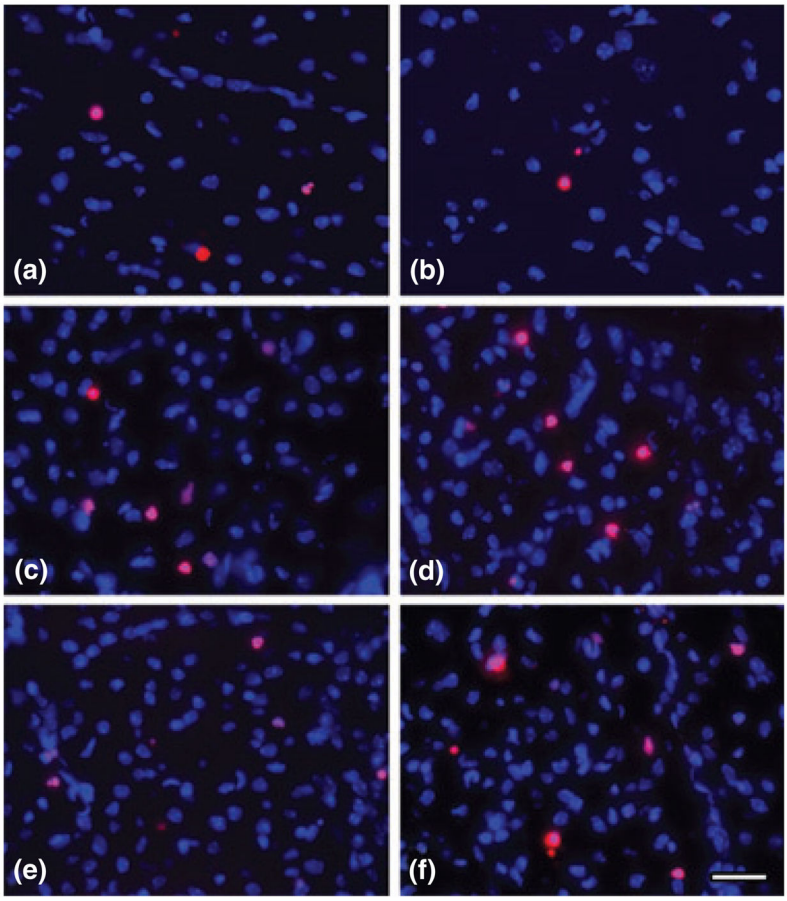

Fig. 3.

Levels of apoptosis are independent of caspase 12 activity in *Plp1* mutants. Cervical spinal cords from (a) *X/Y* (b) *Caspase 12*$^{-/-}$: *X/Y* (c) *msd/Y* (d) *Caspase 12*$^{-/-}$: *msd/Y* (e) *rsh/Y* and (f) *Caspase 12*$^{-/-}$: *rsh/Y* were labeled by TUNEL (red) and DAPI (blue). Numbers of TUNEL-positive nuclei are increased in *msd/Y* and *rsh/Y* single and double-mutant mice compared with *X/Y*. Scalebar: 50 μm.

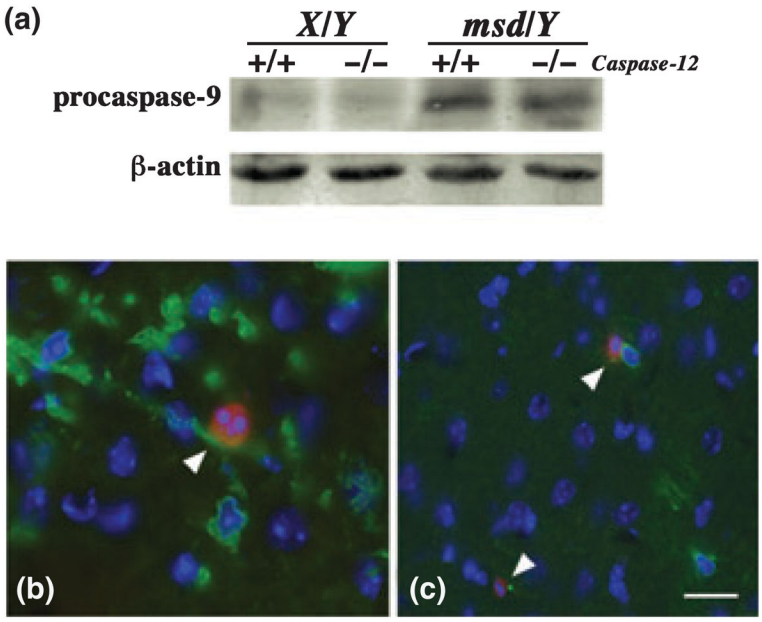

Fig. 4.

Caspases downstream of caspase 12 are activated in *Plp1* mutant mice. (a) Western blots show caspase 9 induction in P16 *msd/ Y* and *Caspase 12*$^{-/-}$: *msd/Y* spinal cords (b,c) Immunolabeling for PLP1(green) and activated caspase 3 (red) in brains from (b) P16 *msd/Y* and (c) *Caspase 12*$^{-/-}$: *msd/Y* show that caspase 3 is activated in the double mutants. Scale bar: 20 μm.

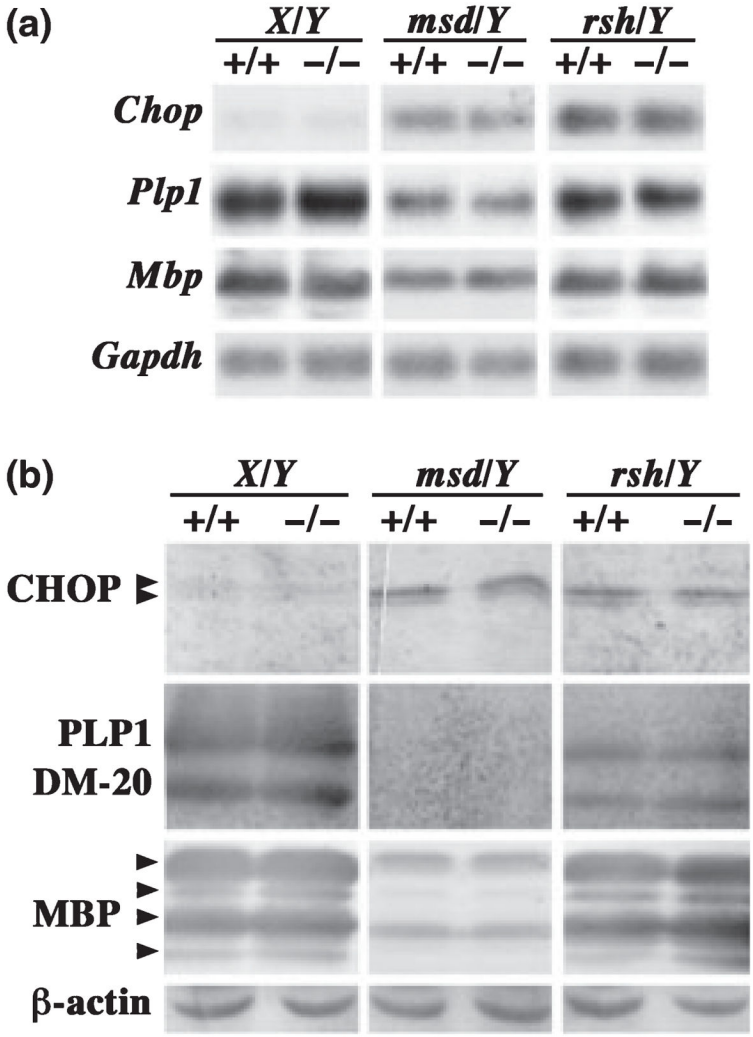

Fig. 5.

Oligodendrocyte function is independent of caspase 12 activity in *Plp1* mutant mice. (a) Northern blots and (b) western blots confirm induction of the UPR marker protein, CHOP, in P16 spinal cords from *msd/Y* and *rsh/Y* mice which is independent of *Caspase 12* expression. Similarly, there are no significant changes in steady state expression of the major myelin proteins PLP1, DM-20 or MBP at the levels of mRNA or protein.

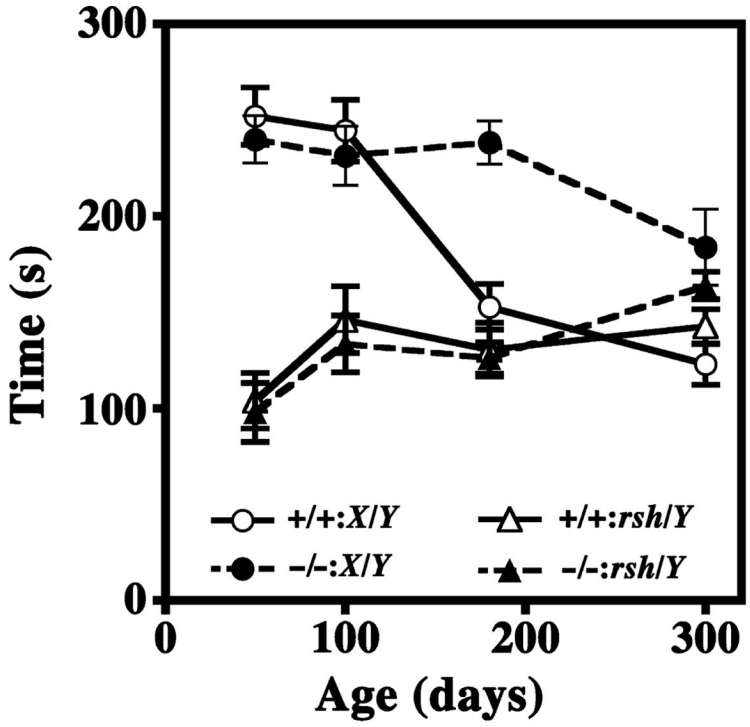

Fig. 6.

Motor coordination is independent of caspase 12 activity in *Plp1* mutant mice. Rotarod analysis at four different ages: P50, P100, P180 and P300. No significant changes in performance are found between *rsh/Y* and *Caspase 12*$^{-/-}$: *rsh/Y* mice. *X/Y* and *Caspase12*$^{-/-}$: *X/Y* initially perform better than the mutants.

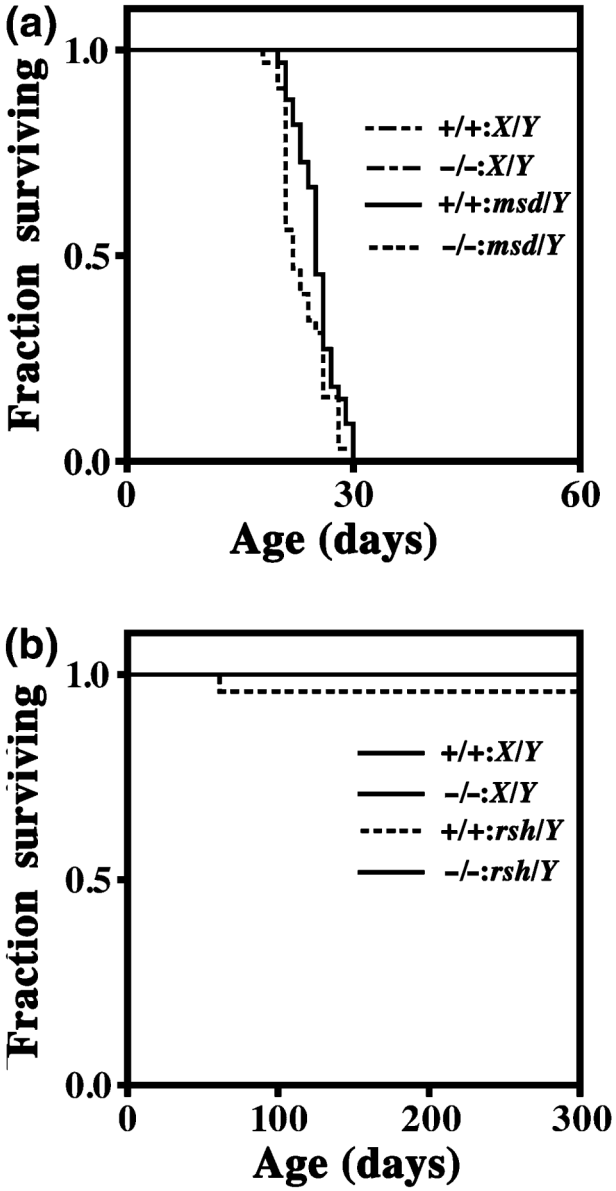

Fig. 7.

Life span of *Plp1* mutant mice is independent of caspase 12 activity. No significant differences in Kaplan–Meier plots from more than 20 mice per genotype for (a) *msd/Y* and *Caspase 12*$^{-}$/$^{-}$: *msd/Y* and (b) *rsh/Y* and *Caspase 12*$^{-}$/$^{-}$: *rsh/Y* mice. *X/Y* and *Caspase 12*$^{-}$/$^{-}$: *X/Y* were killed at 60 days (A) or 300 days (b).

Table 1

TUNEL counts in cervical spinal cord of P16 mice

Genotype	Average TUNEL counts (mean ± SD)
C12$^{+/+}$ *: X/Y*	13 ± 3
C12$^{-/-}$ *: X/Y*	20 ± 6
C12$^{+/+}$ *: msd/Y*	74 ± 7
C12$^{-/-}$ *: msd/Y*	78 ± 6
C12$^{+/+}$ *: rsh/Y*	37 ± 4
C12$^{-/-}$ *: rsh/Y*	42 ± 4

Table 2

DEVDase activity in optic nerve from P16 mice

	Fold-change/mg protein over *C12*$^{+/+}$: *X/Y* (mean ± SD)	
Genotype	**DEVD substrate**	**DEVD substrate + inhibitor**
C12$^{+/+}$: *X/Y*	1.0	1.0
C12$^{-/-}$: *X/Y*	1.2 ± 0.16	1.1 ± 0.38
C12$^{+/+}$: *msd/Y*	5.0 ± 0.98	0.15 ± 0.04
C12$^{-/-}$: *msd/Y*	4.6 ± 0.59	0.52 ± 0.34
C12$^{+/+}$: *rsh/Y*	4.9 ± 0.90	0.60 ± 0.19
C12$^{-/-}$: *rsh/Y*	4.2 ± 0.23	0.47 ± 0.29